

# Novel Fundus Image Preprocessing for Retcam Images to Improve Deep Learning Classification of Retinopathy of Prematurity

Sajid Rahim  
Dept of Computing and Software  
McMaster University  
Hamilton, Canada  
[rahims9@mcmaster.ca](mailto:rahims9@mcmaster.ca)

Dr Mark Lawford  
Dept of Computing and Software  
McMaster University  
Hamilton, Canada  
[lawford@mcmaster.ca](mailto:lawford@mcmaster.ca)

Dr. Kourosh Sabri  
Dept of Ophthalmology  
McMaster University  
Hamilton, Canada  
[sabrik@mcmaster.ca](mailto:sabrik@mcmaster.ca)

Dr Linyang Chu  
Dept of Computing and Software  
McMaster University  
Hamilton, Canada  
[chul9@mcmaster.ca](mailto:chul9@mcmaster.ca)

Dr Anna L. Ells  
Calgary Retina Consultants  
University of Calgary  
Alberta, Canada  
[annaells@mac.com](mailto:annaells@mac.com)

Dr. Alan Wassyng  
Dept of Computing and Software  
McMaster University  
Hamilton, Canada  
[wassyng@mcmaster.ca](mailto:wassyng@mcmaster.ca)

Dr Wenbo He  
Dept of Computing and Software  
McMaster University  
Hamilton, Canada  
[hew11@mcmaster.ca](mailto:hew11@mcmaster.ca)

**Abstract**—Retinopathy of Prematurity (ROP) is a potentially blinding eye disorder because of damage to the eye's retina which can affect babies born prematurely. Screening of ROP is essential for early detection and treatment. This is a laborious and manual process which requires a trained physician performing dilated ophthalmological examination. This procedure can be subjective resulting in lower diagnosis success for clinically significant disease. Automated diagnostic methods can assist ophthalmologists increase diagnosis accuracy using deep learning. Several research groups have highlighted various approaches. This paper proposes the use of new novel fundus preprocessing methods using pretrained transfer learning frameworks to create hybrid models to give higher diagnosis accuracy. The evaluations show that these novel methods in comparison to traditional imaging processing contribute to higher accuracy in classifying Plus disease, Stages of ROP and Zones. We achieve accuracy of 97.65% for Plus disease, 89.44% for Stage, 90.24% for Zones with limited training images.

**Keywords**—Image Pre-Processing; Retinopathy of Prematurity; Deep Learning; Transfer Learning

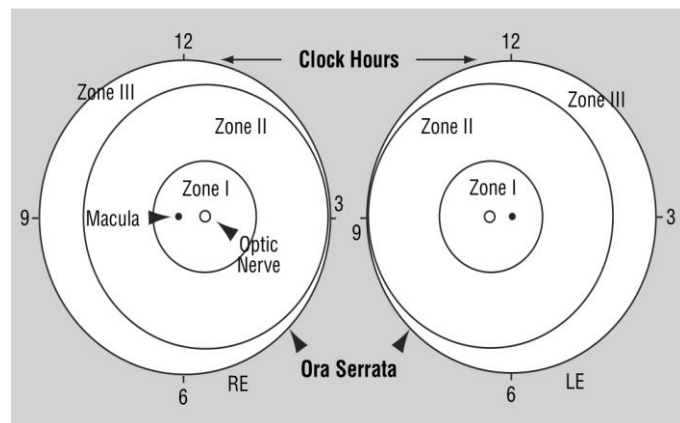
## I. INTRODUCTION

Retinopathy of prematurity (ROP) is a disorder of the developing retinal blood vessels in premature infants and is a leading cause of childhood blindness. In full term infants, ROP does not occur as the retinal vasculature is fully developed. In premature infants, the development of the retinal blood vessels, which proceeds peripherally from the optic nerve during gestation, is incomplete. Hence, the extent of immature development of retina depends on the degree of prematurity, thereby increasing the possibility for abnormal development [1][2].

There are several stages or classification of Retinopathy of Prematurity and is based off schema of retina in both left and right eye (Figure 1). These can be summarized as noted by American Academy of Ophthalmology [3] as follows:

- i. **Location:** **Zone I** – Posterior retina within 60 deg. Circle centered on optic nerve; **Zone II** – from posterior circle (**Zone I**) to nasal ora serrata anteriorly. **Zone III** – remaining temporal peripheral retina. Extent indicates number of clock hours involved.
- ii. **Severity:** **Stage 0** – immature retinal vasculature without pathologic changes. **Stage 1** - presence of demarcation line between vascularized and non-vascularized retina. **Stage 2** - presence of demarcation line having a ridge. **Stage 3** - a ridge with extra-retinal fibrovascular proliferation. **Stage 4** - partial retinal detachment. **Stage 5** - total retinal detachment.
- iii. **Plus disease:** Vascular dilation and tortuosity of posterior retinal vessels in at least 2 quadrants of the eye.

Fig 1. Retina showing zones/hours for location and extent of ROP [4]



Clinical diagnosis remains a challenge area as it requires direct dilated ophthalmologic examination. There are variabilities between experts in diagnosing various stages of ROP. Highly trained specialists able and willing to manage ROP are very few in most countries, which also impacts patients who may be located across a large geographic area. Training of specialists requires time and examining patients presents a challenge given the age of these premature babies. ROP incidents worldwide have been increasing given the improvements of neonatal care and population growth [5][6].

Globally, 19 million children suffer from visual impairment of which 1.85 million are likely to have developed some degree of ROP. For those, diagnosed with ROP, 11 % will have severe visual impairment, and 7 % will have mild/moderate impairment. ROP Incidence rates have been noted as 9% in Developed countries but higher at 11% in Developing countries [5].

Early detection is critical so that appropriate follow ups and treatments can be provided. Goal is to improve patient care by streamlining the screening and staging of patients at risk of ROP. 55 infants examined for every one treated in the UK [7]. ROP is a clinical diagnosis with high rates of interobserver variability. To provide improved quality of care by specialists in being able to remotely diagnose patients can be very beneficial especially in remote locations in Canada and many parts of the world. An automated computer-based image analysis/diagnosis of ROP adds to the support system of early detection. This requires image standardization which is a secondary challenge even though Retcam [8] is preferred pediatric ophthalmological camera system. Some teams have opted to use Smartphone cameras using MilRetCam [9]. Image processing and deep learning classifiers that perform well on one system may fail to perform similarly across different systems. Image quality is a significant challenge with over saturation or illumination. Contributing to image quality is degeneration within fundus image that is resulting from Retcam lens to cornea contact air gaps, reflection from the cornea, vitreous, and retina itself. Once image quality is addressed, fundus pigmentation varies across ethnic and geographic regions and therefore need for validation across each region. One also has the option to decide on the role of deep learning in clinical practice for screening, diagnosis and monitoring post treatment or even using the image preprocessor as an assistive clinical diagnosis tool for tele-health.

The research was inspired by challenging accessible to other researchers as a collective to address this worldwide challenge. This paper demonstrates how novel image processing can a pivotal role when used with deep learning frameworks to build classification system for screening and diagnosing aspects of ROP such as presence of Plus, Stage of ROP and Zones purely based on better processed fundus images. In our research, we prepare 2 deep learning classifiers that separately diagnose Plus disease, Stages of ROP and Zones. The research contributions discussed in this paper include:

1. Image Pre-processing methods which include traditional and new novel methods

2. Two deep learning frameworks that leverage transfer learning
3. Classifier results using traditional and novel image preprocessing methods

The paper is organized in the following sequence starting with Introduction, Background which discusses present research and highlights their gaps, image preprocessing methods and how we organized the datasets, transfer learning approach taken finalizing with comparison of results obtained using various image preprocessing techniques. Future work is also briefly discussed at the end.

## II. RELATED WORK

Recent approaches to ROP and plus disease detection are mostly based on convolutional neural networks (CNN), which take fundus images as input and do not require manual annotation. These show very promising results. Current methods for ROP detection are capable of coarse-grained classification, such as discriminating severe from mild ROP; they do not specifically assess disease stage or zone. While the literature suggests that severe disease rarely develops without changes in posterior pole vasculature, providing additional outputs of the zone and stage could improve the interpretability of the system's assessment and improve performance.

Worral et al. [10] were the first to aim CNN towards ROP. Using approx. 1500 image from 35 patients and 347 exams (2-8 images per eye), they utilized a Bayesian CNN approach for posterior over disease presence; thereafter used a second CNN trained to return novel feature map visualizations of pathologies. Accuracy of 0.918 in terms of identifying eyes with ROP vs healthy eyes with sensitivity=0.825 and specificity=0.983 per eye.

Wang et al. [11] have architected largest automated ROP detection system named DeepROP using Deep Neural Networks (DNNs). Largest dataset at the time utilized (20,795 images, 3722 cases, 1273 patients) with clinical labels done by clinical ophthalmologists. ROP detection was divided into ROP identification and grading tasks using two DNN models namely Id-Net and Gr-Net. First determined if ROP was present, if present, the second graded ROP either as Minor (Zone II/III and Stage 1/Stage 2) or Severe (threshold disease, Type 1, Type 2, AP-ROP, Stage 4/5). Standard imaging technology has been employed with private datasets and inability to reproduce these findings. Images used are of a single population cohorts and pre-processing datasets results are not clearly identified prior to training. Validated against 472 screening from 404 infants resulted in identification of ROP with sensitivity of 84.9%, specificity of 94.9% and accuracy of 95.6% while grading of Minor/Severe with sensitivity of 93%, specificity of 73.6% and accuracy of 76.4%. It outperformed 1 out 3 experts.

Redd et al, Brown et al. [12] Devised a two stage CNN i-ROP-DL which combines prediction probabilities via a linear

formula to compute an ROP severity score, which can serve as an objective quantification of disease; a similar idea could provide finer grading of plus disease. The i-ROP-DL deep learning system is the first to detect specific ROP classifications. 6000 images used and professionally graded to normal, pre-plus, plus ROP stages; partial/full detachment images were excluded. Two stage CNNs were used; first was to segment and other was to classify. The classifier only classified plus disease and solution is acknowledged by authors limited in handling one type of imaging source. 91% accuracy with sensitivity and specificity of 93%, 94% for Plus disease and 100%, 94% for Pre-plus or worse was achieved. This outperformed 6 out of 8 ROP experts.

Mulay et al [13] focused detection of demarcation line using CNN based model Mask R-CNN such that ROP Stage 2 can be detected better. Image preprocessing is used to overcome poor image quality; detection accuracy was 88% with positive predictive value of 90%/75% and with negative predictive value of 97%/42% in terms of sensitivity/specificity. This validated that image preprocessing assists deep learning classification. Vinekar et al. [14] used deep learning utilizing 42,000 images from a tele-ROP screening in India with the goal of detecting presence of Plus disease. Using two test sets which excluded pre-plus disease, they were able to achieve 95.7%/99.6% and 97.8%/68.3% in terms of sensitivity/specificity.

Tong et al. [15] architected another novel approach to identifying ROP and its stages using 2-layer CNN DL and predict lesion location in fundus images. Datasets of over 36,000 Retcam images were reviewed and labelled by 13 ophthalmologists with 10-fold cross validation (9 training, 1 testing). Each image tagged with a classification (ROP severity) and identification label (ROP clinical stage). Normal when no abnormalities, mild for Stage 1/Stage 2 without plus disease; semi-urgent for Stage 1/Stage 2 with plus disease, urgent for Stage 3, Stage 4, and Stage 5 with or without Plus disease. Very basic preprocessing which included adding noise and brightness to images was performed, dataset then augmented for volume and image compressed. Resnet 101 CNN using transfer learning was used for classification and Faster R-CNN was used to identify ROP stage, presence of Plus disease and predict objective boundary of lesions. Very good accuracy has been achieved by using transfer learning of 0.883, 0.9, 0.957 and 0.87 for normal, mild, semi-urgent and urgent were achieved with additional accuracy of Stage and Plus disease at 0.957 and 0.896. A repeat without transfer showed poor sensitivity and accuracy.

Wu et al. [16] developed 2 deep learning models to demonstrate deep learning (DL) system can be used to predict the occurrence and severity of ROP. Two models were specifically designed to look for presence and severity of ROP using ResNet50. Severity was defined as mild: Type II ROP, Zone II Stage 1, Stage 2 ROP without plus disease and Zone III Stage 1,2, or 3 ROP with severe: Stage 4 or 5 ROP, Type I or aggressive posterior ROP. Results for presence of ROP was 100%/38% and severity of ROP being 100%/47% in terms of sensitivity/specificity. Here too image preprocessing was not highlighted as having been used.

Ding et al. [17] Proposed a hybrid architecture focused on localization of demarcation line and in parallel feeding a black and white reciprocal image as 2 channel input; former provides a feature input of interest area. It is fed into traditional CNN. Paper conducts experiments using 2759 images from local hospital which were classified by stages. Images preprocessed using contrast enhancing features. Preprocessed image is used for object segmentation by applying Mask R-CNN to highlight demarcation line at pixel level and generate interest bounding box around area of interest creating a binary mask for demarcation line. Transference learning was used to prevent over-fitting; Inception v3 pre-trained on ImageNet was used for classification. Stage 1, 2 and 3 classifications achieved was 0.77/0.78, 0.62/0.61, 0.62/0.62 in terms of sensitivity/specificity. Of significance is ability to detect between Stage 1 and 2.

Zhao et al. [18] turned to deep learning for identifying Zone I by using Retcam images. Their approach is based on firstly identifying position of optic disc and macula; thereafter center point of optic disc and macula calculated from which Zone 1 is then calculated. This is the only study we know of that identifies Zones (I), They can achieve accuracy of 91% with IOU threshold of 0.8. They acknowledge that disc and macula positioning is required without which this study is incomplete. An automated Zone Quality Filter is a good addition.

The comprehensive review above shows promising results but also note many gaps which were very similar. All made use of non-public standardized and non-independently verified datasets private datasets which challenges reproducibility; there remains a strong need to have a standardized ROP data for this work. Diversity of population cohorts remains a challenge to address the geographical diversity to address this as a worldwide challenge that is open and available for independent non-profit work. Such standardized ROP dataset will also allow for reproducibility of published works.

Fundus images were taken from various types of cameras with differing resolutions. Hence fundus image pre-processing is a core requirement for yielding standardized elevated features images that support a high degree of accuracy; most used basic image pre-processing prior to running the classifiers. This did happen in some cases but was given a low priority or not used in others. All authors have kept their application details private and there is not enough information to allow for a detailed peer review. Lastly there is no consensus on standardized outcomes expected – most use multi-class classifications to denote a condition making it more difficult to replicate or reach consensus. With this in mind, we focused on finding the optimal fundus preprocessing techniques that can enhance overall features pertinent in providing best classifier outcomes in terms of Plus, Stage and Zone; this can be regarded as one of the major contributions in this research.

### III. FUNDUS PREPROCESSING

Fundus Image pre-processing can be defined as either the extraction, enhancing, or removal features within the image

which can include pixel brightness and geometric transformations [19]. Also known as image domain, this is most widely used due to its simplicity. The second class of method can be categorized as restoration.

#### A. Image domain methods

Fundus Image pre-processing, is needed to normalize image brightness, correct for image non-uniformity, reduce noise or image artefacts such that image clarity is restored. Fundus images are challenged significantly with noise that includes reflection, artifacts and out of focus capturing. Some conventional feature-based techniques for preprocessing include Gray scale Conversion, Contrast Limiting Adaptive Histogram Equalization (CLAHE) [19], and Image filtering [23][24].

There are two primary methods which is widely used in fundus image preprocessing. The first being gray scale using green channel and second being Contrast Limited Adaptive Histogram Equalization (CLAHE) [19]. CLAHE has most improvements over Histogram Equalization (HE) [20][21] and Adaptive Histogram Equalization (AHE) [22] computes several histograms for different sections of the image, and subsequently distributes the lightness values but it caps the histogram to a predefined value to prevent over amplification that occurs with AHE; this results in low noise sharpened image which can assist in numerous medical diagnoses [25][26][27][28]. CLAHE and Gray Scale via green channel due to their simplicity and effectiveness has been used in many variations such has been used within ophthalmological settings for wide range of applications such as Diabetic Retinopathy classification [27][28]. CLAHE is very versatile and it includes its implementation to includes LAB color space but as noted in [32], we also found it over illuminated ROP images and was not considered as viable. Overall, the core challenge of restoration of ROP fundus image remains due to haziness from internal reflection.

#### B. Restoration methods

When light enters the retina, it not only undergoes refraction prior to hitting the retina; it also reflects from each layer it hits including sclera, lens, vitreous and retina itself. This reflection contributes a significant amount of noise. The formation of haze image is noted. Model for describing formation of haze is noted in atmosphere as [30]:

$$\mathbf{I}(x) = \mathbf{J}(x)t(x) + \mathbf{A}(1-t(x)), \quad (1)$$

Where  $\mathbf{I}$  is observed intensity,  $\mathbf{J}$  is scene radiance,  $\mathbf{A}$  is global atmospheric light, and  $t$  is the medium transmission describing the portion of light reaching camera un-scattered. We attempted in our study to leverage atmosphere based de-hazing methods using Dark Prior Channel as described first by He et al. [29] against each fundus image. It is based on observation that in haze free outdoor image, one of the channels will have a patch with low value. Haze removal is performed by estimating the transmission, refining of the

transmission by soft matting, final scene radiance recovery and finally estimating the atmospheric light that of the highest intensity in input image. While good for terrestrial use, this did not yield much success for ROP fundus images. Similarly other dehazing powerful techniques as proposed by Zhu et al. [30], and Sami et al. [31] were also reviewed without success for improving ROP Retcam images in terms of details.

Gaudio et al. [32] proposed Pixel Color Amplification (PA) which enhanced fundus images using amplification theory based on Dark Prior Channel (DCP) theory. DCP theory permits inversions which can be used to derived additional Priors namely Inverted DCP (Illumination Correction), and Bright Channel Prior (Exposure Correction) – a *fourth* novel Prior based on inter-relationship of 3 is derived by Gaudio et al. This provides enhancement methods for controlling brightness denoted by letters A, B, C, D; for darkness letters WXYZ. These letters can be prefixed with  $s$  to provide sharpening of retinal features. Pixel Amplification showed good retinal enhancement for EYEPACs/IRID; this held good promise with some modification for ROP fundus images.

Zhang et al.[33] highlight the problem of reflection specific to a retina by considering system of capturing as a reflective/illuminative imaging system and recognizing image formation as a multi-layer model. Transmission term which He, Gaudio and others fix a constant value; is applied to illuminating light but also reflected light. First part estimating enhanced restoration image value using illumination, transmission of lens and scatter matrix. Second part restores the image by focusing on retinal area ignoring black exterior box; coarse illumination correction is performed across red, green, and blue channels followed by fine illumination boosting where gray scale dark channel prior is used for dehazing. The last step is scatter suppression which results in an illumination corrected and dehazed image. The method is called Double Pass Fundus Reflection (DPFR). We find this of high significance for ROP fundus preprocessing and it aligns with our analysis of Retcam images that reflection is a principal cause of quality challenge. for ROP, we enhance it further. To make it more suitable for ROP Retcam, there were some features in guided filter and finer correction which we changed to make it suitable for Deep Learning usage and denote this as DPFRr.

In our research, we employed both image domain and restoration methods; in the later we improved some aspects that make them more suitable for deep learning classifiers for ROP.

## IV. DATASET AND METHODS

#### A. Architecture Pipeline

Our architecture as labelled ‘McROP’, is described in **Fig 2**. It has 5 core components; starting with Labelled ROP datasets for Training and Validation for Plus, Stage, and

Zones; this is fed into Image Preprocessing where each distinct dataset is created for each technique e.g Gray Scale to DPFRr-CLAHE. These paired datasets move forward Image resizing into 224x224 pixels. Data augmentation is the last step prior to enabling the separate ROP classifiers to produce Class results for ROP – Plus Disease, identify Stages, and Zones.

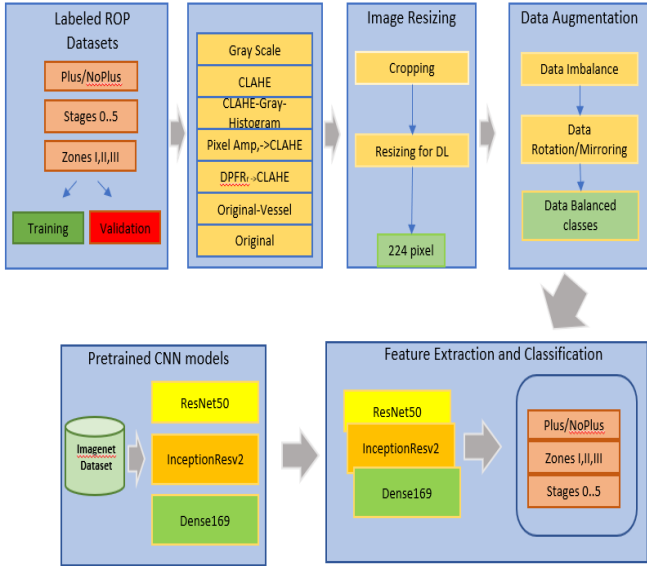


Fig 2. McROP Framework

### B. Dataset Preparation

Dataset of Retcam fundus images of ROP patients were obtained as part of collaboration agreement with University of Calgary. Original images were captured by the RetCam imaging system in collaboration with a hospital. The original images were  $640 \times 480$  which were then resized to 224x224 prior to classifier processing. Ground truth was available and rechecked and where different, another ground truth was noted. Data quality guidelines were identified such as bad focused images, over illuminated, retina features required were not available or too many external reflections were excluded. Image of the exterior of the eyes were also excluded. Data Quality Filter is considered as part of our future work contribution.

Three separate datasets were created; one each for Plus diseases (Pre-plus was excluded), Stages, and Zone classification. 8:2 split for Stage/Zone with approx. 9:1 split for Plus was performed for training and validation subsets. The split also ensured that data from the same patient's did not appear in the validation from same eye; alternate eye was used if required as a replacement. Total of 29 patients with up to 9 visits; bilateral images of up to 6 images per visit. Selection for Plus disease was made by the specialists which ensured optic disc, and vasculature was visible. For Stage, the image may have optic disc visible and/or the periphery where the

demarcation line may or may not be present. For Zone, the criteria was stricter, the peripheral area must be present as well as the optic disc and macula; both must be present in order to be able to provide an assessment; this is also in line with Zhao et al. [18].

A parallel dataset for Stage was created; In this method, the aim is to reduce the noise from other aspects of the fundus image such as blood vessels. For this, we turned to U-Net[35] segmentation as already there is a large body of knowledge where we could leverage this from. Choice was made of LWNET[36] which is a minimal model segmentation design. It has ability to generate both coarse and fine vessel segmentation; we just used the coarse segmentation as proof of concept. Using pretrained model, we passed entire training/validation datasets to create respective segment map; blood vasculature pixels were then erased using average colour of adjacent region using coarse square of 32 and then scaling downwards to 4 pixels. More future work is still required as the colour value causes it to still be visible in DPRFr in conjunction with Mask R-CNN segmentation.



Fig 3. Fundus image, LWNET generated vessel map, post erasing

### C. Preprocessing Methods

At this point, all data is now correct and labelled into training and validation datasets. We now look at 6 preprocessing algorithms that will be employed to generate 6 datasets for each preprocessing method. First was baseline without any preprocessing. Extensive use is made of OpenCV library [38][39] for using Gray scale conversion from colour, CLAHE with cliplimit of 2.0 and applied to each channel then merged, a merged process of CLAHE (3 channels) into Green Channel into Histogram Equalization (CGH), Pixel Colour Amplification (PA), Pixel Amplification into CLAHE (PA-CLAHE), Double Pass Fundus Reflection modified for ROP (DPFRr) and DPFRr into CLAHE (DPFRr-CLAHE). At this point all the images remain in  $640 \times 480$  format. For each process, we have now standardized the preprocessor images for training and testing. **Fig 3.** shows sample of pre-processed images from each of these methods.

Original image is used as first method to establish a baseline. Gray scale is performed to void any unique colour uniqueness that cause model to pick additional characteristics. Denoted by standard formula:

$$\mathbf{Io} = ((0.3 \times \mathbf{R}) + (0.59 \times \mathbf{G}) + (0.11 \times \mathbf{B})), \quad (2)$$

CLAHE is used to enhance the overall contrast of the image and smooths out the pixels; this represents most common used method for fundus-based DL CNN use. We then proceed to extend another dataset using CLAHE by applying Green Channel only as it carries most information; on this Histogram Equalization is applied - this represents high level of signal for identifying demarcation line visually while keep other noise balanced.

Pixel Colour Amplification (PA) by Gaudio et al. [32] is an open-source image enhancement toolkit which uses 4 letters A-D to brighten/and 4 letters W-Z to darken including sharpening; these can be combined to form an average. Standard best method which works for ROP images is A,C,X; presently this is controlled via choice of parameters - we extend this process to autodetect the illumination of original image and apply the correct methods. For ROP images, it tended to highlight the demarcation line well as well as the vasculature. However, it was challenged with oversaturation of reds in the center vision region as described by Dissopa et al. [34]; we confirmed this significant challenge in ROP images. Hence to balance the illumination and contrast in post PA image, we extended this output into CLAHE model to yield PA\_CLAHE dataset which is more balanced overall.

DPFR[33] is latest novel technique which takes into account the image capturing mechanism which includes illumination, its forward journey into the eye and reflection; the transmission index is also estimated and not fixed as in Pixel Amplification. Final image  $\mathbf{S}$  is computed using the sum of two back scattering components  $\mathbf{R}_0$  from retina and  $\mathbf{R}_1$  being from intra-ocular.

$$\mathbf{S}(\mathbf{r}) = \mathbf{R}_0 + \mathbf{R}_1 = \mathbf{I}_{\text{ill}}(\mathbf{r}) \cdot \mathbf{T}_{\text{lens}}(\mathbf{r}) \cdot [\mathbf{T}^2 \mathbf{I}_{\text{sc}}(\mathbf{r}) \cdot \mathbf{O}(\mathbf{r}) + 1 - \mathbf{T}_{\text{sc}}(\mathbf{r})], \quad (3)$$

Restoration of image  $\mathbf{O}$  is implied if illumination matrix  $\mathbf{I}_{\text{ill}}$  and transmission matrix  $\mathbf{T}_{\text{lens}}$  and  $\mathbf{T}_{\text{sc}}$  can be measured using ‘prior’ which is a pre-known information. By estimating  $\mathbf{I}_{\text{ill}}$ ,  $\mathbf{T}_{\text{lens}}$  and  $\mathbf{T}_{\text{sc}}$  and solving Eq. (2) an enhanced version is  $\mathbf{O}$  obtained. The original method has image preprocessing, coarse followed by fine illumination, and scatter suppression. The resulting image is very grainy when viewed closely for ROP use; two main improvements were made to reduce the graininess namely in the guided filter and dehazing estimation and hence we refer to it as DPFRr. The changes also reduce the level of choroidal vessels which become visible. Hence the use of LWNET [36] to level out larger vasculature assists further.

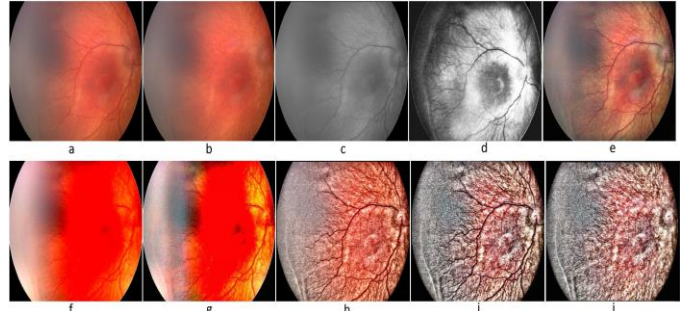


Fig 4. Original, vessel removal, gray scale, CGH, CLAHE, PA, PA\_CLAHE, DPFRr, DPFRr-CLAHE, DPRFr-vessel removed (a-j).

#### D. Data Resize and Augmentation

We resize the training/validation images by first cropping the images to maximize circular region. Resizing is a critical component [38] in Deep Learning especially in ROP for Stage/Zone classification. Resizing implies image transformation [38] and OpenCV[38][39] which is widely used provides resize function with several choice of filters such as nearest, bilinear, bicubic and lanczos. The most optimum choice we observed was lanczos filter that uses a truncated sinc applied on 8x8 neighborhood. We found it most effective resizing method in retaining information from original information such as vessels, OD, macula, demarcation line next to bicubic method. We resize the pipelined images from each of preprocessed methods as noted in section IV.C. to 224x224 pixels RGB images using OpenCV resize with lanczos method. Additional benefits of the resizing is the smoothing effect especially for DPFRr.

As our ROP data was not sufficient, we utilized data augmentation which was performed with several methods including rotation of 90 degrees, flipping left/right, up/down with each change in orientation being treated with scaling intensity, contrast including gamma and sigmoid, saturation, gamma, hue. This yielded up to 50 images. Each image is a variation of original image. The multiple was altered to ensure we get close enough balanced set thereby using weights in the classifier to mitigate overfitting. Extensive use of OpenCV library of image processing methods [38][39] were used.

Below tables show ROP Datasets for Stage, Plus and Zones.

TABLE I. ROP DATASETS

	Stage Dataset		
	Training	Augmented Training	Testing
<b>Stage 0</b>	71	3905	15
<b>Stage 1</b>	47	2585	9
<b>Stage 2</b>	101	4040	20
<b>Stage 3</b>	85	3400	14
<b>Stage 4</b>	3	165	1
<b>Stage 5</b>	2	110	1
	<b>309</b>	<b>14205</b>	<b>60</b>

## V. EXPERIMENTS

	Plus Disease Dataset		
	Training	Augmented Training	Testing
No plus	855	8550	72
Plus	61	6039	13
<b>916</b>	<b>14589</b>	<b>85</b>	

	Zones Dataset		
	Training	Augmented Training	Testing
Zone I	11	539	3
Zone II	143	5005	33
Zone III	19	931	5
<b>916</b>	<b>6475</b>	<b>41</b>	

### E. Classifiers

We utilized ResNet50[40], InceptionResv2[41], Dense169[42] which had been pre-trained using ImageNet and provided by Keras [43]. In all cases, we don't want last fully connected layer; this is replaced by our task for Plus, Stage and Zone. We freeze the weights of each model to false to stop updates to pretrained weights as we want to preserve knowledge retained earlier using ImageNet dataset. We add custom block of CNN layers on top of each one of these models to build a hybrid model. Transfer Learning [43] has been successfully used to improve classifiers [26][27][28] and is critical as the number of ROP images is limited. It is helpful when there is not sufficient data to train full model as it prevents overfitting and aids in the training process. The shape of each pretrained model's input layer and final dense layer is modified. Weights are additionally calculated based on number of training images to prevent overfitting; this included L1 regularizer and Dropout were also employed to prevent overfitting. Use was made of GradCam[44] to check for features being considered.

For Plus, Stages, and Zones, in ResNet50, we allow 'res5c\_branch2b', 'res5c\_branch2c', 'activation\_97' layers to be trainable but freeze the rest. For ResNet50 (Plus, Stages, Zones), we add fully connected layer GlobalMaxPooling2D, Dense(1024, 'relu', 11), Dropout(0.2), Flatten, Dense(1024, 'relu', 11), Dropout(0.2), Batchnormalization and final classifier for Plus, Stages, Zones using softmax activation function.

For InceptionResv2 (Plus, Stages, Zones), we also freeze all layers except 'block8\_10\_mixed' which is trainable. For Plus, add fully connected layer using Flatten, Dense(1024, 'relu'), Dropout, Dense(1024, 'relu'), Dropout, Batchnormalization with final classifier for Plus using softmax activation function. For Stages and Zone, they share same model as defined in add our fully connected layer (Flatten, BatchNormalisation, Dropout, Dense(1024, 'relu', 11), Dropout, Dense(1024, 'relu', 11), Dropout, Batchnormalization and final classifier for Stage using softmax activation function. Dropout rate for Stages and Zones is 0.7 and 0.2 respectively.

A standardized set of models were prepared for Plus, Stage and Zone. A self-adjusting training rate was added with start rate of 1e-5 which is called by LearningRateScheduler, batch size of 32, epochs of 10, Adam optimizer, patience of 5 early stop Inference rate was set at standard 0.5. Early stopping was employed by monitoring the validation loss.

These experiments were conducted on T5810 workstation with Xeon 10 core CPU, 96gb memory and RTX3060 12Gg GPU card with python 3.9, Keras 2.9, Tensorflow 2.9 with GPU support and CUDA 11.3.

Experiments were arranged in the order of Plus, Stage, and Zone classifiers. For each, a series of 8 datasets were created namely original (baseline), Gray scale, CGH, PA, PA-CLAHE, DPFRr, DPFR-CLAHE. For each dataset (training, validation), we ran 2 classifiers namely ResNet50 and InceptionResv2; if required Dense169 was run to verify any outliers. This was to ensure that results were replicable, and no anomaly was entering the results. Also, it would pave the way for ensemble framework as our later work contribution.

The results from our system are as follows for each classifier and method of preprocessing is shown below. Tables II, III and IV show ResNet50, InceptionResv2 results for Plus, Stage and Zones. In Plus disease, and Stage classification DPFRr shows best outcomes while in Zone classification, DPFRr-CLAHE gives best results in terms of highest sensitivity/specificity. The highest achieved result is broken down in Table V, VI, VII in No Plus/Plus, Stage 0-5, and Zone I-III with the confusion matrix respectively.

TABLE II. PERFORMANCE OF RESNET50, INCEPTIONRESV2 FOR PLUS

PLUS	ResNet50						InceptionResv2					
	Precision	Recall	Kappa	F1	AUC	Final Score	Precision	Recall	Kappa	F1	AUC	Final Score
Base	91.76	91.76	83.52	91.76	98.35	91.21	97.64	97.64	95.29	97.64	99.41	97.45
Gray	95.29	95.29	90.58	95.29	99.28	95.05	97.65	97.65	95.29	97.64	99.52	97.49
CLAHE	95.29	95.29	90.58	95.29	99.39	95.09	97.65	97.65	95.29	97.64	99.52	97.49
CGH	91.76	91.76	83.52	91.76	98.85	91.38	96.47	96.47	92.94	96.47	99.37	96.26
DPFRr	<b>97.65</b>	<b>97.65</b>	<b>95.29</b>	<b>97.64</b>	<b>99.88</b>	<b>97.61</b>	<b>97.65</b>	<b>97.65</b>	<b>95.29</b>	<b>97.64</b>	<b>99.64</b>	<b>97.52</b>
DPFRr-CLAHE	<b>97.65</b>	<b>97.65</b>	<b>95.29</b>	<b>97.64</b>	<b>99.91</b>	<b>97.61</b>	<b>97.65</b>	<b>95.65</b>	<b>95.29</b>	<b>97.64</b>	<b>99.86</b>	<b>97.6</b>
PA	91.76	91.76	83.52	91.76	97.35	90.88	92.94	92.94	85.88	92.94	97.23	92.01
PA-CLAHE	91.76	91.76	83.52	91.76	96.69	90.66	94.12	94.12	88.23	94.17	97.19	93.18

TABLE III. PERFORMANCE OF RESNET50, INCEPTIONRESV2 FOR STAGE

STAGE	ResNet50						InceptionResv2					
	Precision	Recall	Kappa	F1	AUC	Final Score	Precision	Recall	Kappa	F1	AUC	Final Score
Base	61.54	26.67	30.1	85	83.58	66.25	72.73	58.53	0.5	78.86	79.62	69.49
Gray	65.71	38.33	41.19	86.38	85.88	71.15	66.66	10	13.63	84.16	86.2	61.33
CLAHE	72.22	43.33	47.61	87.77	86.34	73.91	88.88	26.66	36.11	87.22	87.62	70.32
CGH	65.62	34.99	38.52	86.11	84.63	69.75	66.66	23.33	28.37	85.27	82.71	65.45
DPFRr	63.41	43.33	43.89	86.38	85.74	72	<b>69.64</b>	<b>64.99</b>	<b>60.95</b>	<b>89.44</b>	<b>88.09</b>	<b>79.49</b>
DPFRr-CLAHE	59.64	56.66	50	86.38	82.44	72.94	<b>66</b>	<b>61</b>	<b>56.87</b>	<b>88.33</b>	<b>87.78</b>	<b>77.65</b>
PA	51.72	50	41.21	83.88	86.9	76.66	69.23	15	19.9	84.72	82.17	62.26
PA-CLAHE	<b>63.63</b>	<b>58.33</b>	<b>53.44</b>	<b>87.5</b>	<b>85.95</b>	<b>75.63</b>	56.14	53.33	45.91	85.27	79.91	70.36

TABLE IV. PERFORMANCE OF RESNET50, INCEPTIONRESV2 FOR ZONE

ZONE	ResNet50					InceptionResv2						
	Precision	Recall	Kappa	F1	AUC	Precision	Recall	Kappa	F1	AUC	Final Score	
Base	82.05	78.05	70.37	86.99	90.63	82.66	72.73	58.53	0.5	78.86	79.62	69.49
Gray	70.73	70.73	56.09	80.48	85.48	85.93	58.62	41.46	28.94	70.73	60.29	53.32
CLAHE	80	78.04	68.71	86.17	89.67	81.52	73.17	60.52	38	73.17	75.13	62.27
CGH	76.96	73.17	62.96	83.73	88.37	78.35	58.54	76.77	45.28	76.42	76.76	66.15
DPRFr	75	73.17	61.34	82.92	89.32	77.86	60	51.22	35.44	72.35	68.97	58.92
DPRFr_CLAHE	85.36	85.36	78.04	90.24	94.64	87.64	63.63	51.21	38.46	73.98	71.53	61.32
PA	75.6	75.6	63.41	83.73	91.61	79.58	56.75	51.21	32.5	70.73	73.94	59.05
PA_CLAHE	78.37	70.73	62.5	83.73	90.74	78.99	64.1	60.98	44.44	75.6	73.85	64.63

TABLE V. TOP CLASS BREAKDOWN FOR PLUS CLASSIFICATION

Type	Features	Specificity	Sensitivity	Accuracy
No Plus	No presence of Plus disease	1	0.97	97.65%
Plus	Presence of Plus Disease	0.85	1	97.65%
	Final detection rate	0.98	0.98	97.65%

Confusion Matrix – Plus Disease		
		Plus
No plus		0
Plus	2	11

TABLE VI. TOP CLASS BREAKDOWN FOR STAGES CLASSIFICATION

Type	Features	Specificity	Sensitivity	Accuracy
Stage 0	No Stage disease	0.93	0.67	86.67%
Stage 1	Presence of demarcation line	0.33	0.38	80.00%
Stage 2	Presence of ridge	0.55	0.73	78.33%
Stage 3	Ridge with additional features	0.79	0.73	88.33%
Stage 4	Partial Detachment	0	0	0.00%
Stage 5	Total Detachment	0	0	0.00%
	Final detection rate	0.70	0.65	89.44%

Confusion Matrix – Stage							
		Stage 0	Stage 1	Stage 2	Stage 3	Stage 4	Stage 5
Stage 0	14	1	0	0	0	0	
Stage 1	3	3	2	1	0	0	
Stage 2	3	4	11	2	0	0	
Stage 3	1	1	1	11	0	0	
Stage 4	0	0	0	1	0	0	
Stage 5	0	0	1	0	0	0	

TABLE VII. TOP CLASS BREAKDOWN FOR ZONES CLASSIFICATION

Type	Features	Specificity	Sensitivity	Accuracy
Zone I	Presence of disease in Zone I	1	0.97	95.24%
Zone II	Presence of disease in Zone II	0.94	0.87	83.33%
Zone III	Presence of disease in Zone III	0	0	0.00%
	Final detection rate	0.85	0.85	90.24%

Confusion Matrix – Zone			
		Zone I	Zone II
Zone I		2	1
Zone II	0	33	0
Zone III	0	5	0

With the limited dataset, extensive use of transfer learning, and augmentation of the training dataset, all three classifiers demonstrate that ROP classifiers can benefit from the use of the two novel image pre-processors which can be used on their own or in conjunction with CLAHE/other. With Plus disease, we did not see much difference and refer to F1 score as a factor to differentiate the better of all. In our tests, we repeated the experiments 5 folds; DPRFr yielded the best results overall accuracy of 97.65%.

$$F1 = 2 * (\text{Precision} * \text{Recall}) / (\text{Precision} + \text{Recall}) \quad (4)$$

In terms of Stage disease, we were challenged with not having a large-scale ROP dataset with each cases especially for Stage 4, and 5. In our study, we do not combine multiple conditions to bundle Stage, Zone or Plus; instead we aim specific at the studying the impact preprocessing has on ROP classifiers. We find DPRFr gave best sensitivity with a higher specificity of 65%/70% with overall accuracy of 89.44%. When this is broken down for Stage, it is observed that this provides a high sensitivity/specificity for Stage 3 followed by Stage 2 and Stage 0. Stage 1 is challenged – this is primarily due to the very fine grainy output which even though reduced significantly does cause challenge in detection. This is a future work of improvement.

While Zone classification is a challenge to identify, we took the opportunity once again attempt this as a proof of concept. The criteria for Zone eligible image is very stringent and a Data Qualifier process may be a valuable contribution to this body of knowledge. In our results, it was rather interesting to observe DPRFr-CLAHE also worked well here too and identified Zone I/II with very high sensitivity/specificity and overall accuracy of 90.24%. In terms of Zone I detection, it shows higher accuracy of 95.24%, and Zone II with 83.33% accuracy. This is better than 91% as was noted by Zhao et al.

[18] for Zone I only. This is as we are aware of the only paper where Zone I and II have been showed to be classified successfully using deep learning. Zone III was challenge due to lack of sufficient data.

## VI. CONCLUSION AND FUTURE WORK

The main contribution of this paper is to validate image preprocessing that improves the accuracy of deep learning CNN created for ROP detection for Plus, Stage, and Zone. We extended traditional methods by improving two novel image methods and combining them with traditional methods; this accentuate ROP features and improves the accuracy of deep learning classifiers. We leveraged transfer learning with pretrained models and constructed 3 classifiers for classifying Plus, Stage1-5 and Zone separately. Though our experiments, we showed that the preprocessing techniques and transfer learning can result in significantly improved accuracy. This paper is also the first as we are aware that studied ROP Plus, Stage and Zone detection purely from image pre-processing and deep learning based on transfer learning.

To further improve the detection and accuracy, we propose a number of changes specifically to create hybrid approach using Pixel Amplification and DPFRR, and secondly to use Mask R-CNN to segment fundus image to isolate non-vascular region where a demarcation line may be present. This with further segmentation of OD may then be used for Zone III detection. Our classifiers for Plus, Stage, Zone may also be combined as a multi-instance classifier using ensemble techniques. These novel methods should also be reviewed if they may also qualify prior disqualified images using traditional image pre-processing methods which were removed for quality reasons to be re-included and therefore increasing the training/validation dataset. Lastly, there is a need for Data Quality Filter process for Plus, Stage and Zone to automatically assess images to a prescribed agreed upon standard across ROP community including an open ROP standardized dataset with labelled ground truth. We hope to contribute to these aspects in future works.

## ACKNOWLEDGMENT

Sajid Rahim recognizes his co-supervisors, Dr Kourosh Sabri, Pediatric Ophthalmologist/Professor of Medicine at McMaster Children's hospital who brought in specialized insights into this pediatric challenge and Dr Anna Ells, University of Calgary for supporting this study by making available ROP dataset. He also acknowledges and thanks Alex Gaudio[32] for detailed blackboard deep discussions in fundus image processing. Dr David Wong, Head of Ophthalmology/Professor of Medicine (University of Toronto) at St. Michael's Hospital, Toronto who triggered the idea to study deep learning applicability for retinal diseases.

## REFERENCES

- [1] Walter M. Fierson, "Screening Examination of Premature Infants for Retinopathy of Prematurity" American Academy of Pediatrics, Online, 2018.
- [2] AMMA, "Screening Examination of Premature Infants for Retinopathy of Prematurity" International Committee for the Classification of Retinopathy of Prematurity, Online, 2005.
- [3] Stephen J. Kim, et al., "2022-2023 Basic and Clinical Science Course, Section 12, Retina and Vitreous", American Academy of Ophthalmology, Dec 2022.
- [4] Jefferies AL, et al. "Retinopathy of Prematurity: An update on screening and management." Canadian Pediatrics Society , Online: <https://www.cps.ca/en/documents/position/retinopathy-of-prematurity-screening>, Aug 2019.
- [5] Sabri K., "Global Challenges in Retinopathy of Prematurity screening: Modern Solutions for Modern Times", PEDIATRICS, Online, Jan 2016
- [6] Quinn G.E., "Retinopathy of prematurity blindness worldwide: phenotypes in the third epidemic", PMC, Online, May 2016
- [7] Haines, L., Fielder, A. R., Scrivener, R., Wilkinson, A. R., & Pollock, J. I., "Retinopathy of prematurity in the UK I: the organisation of services for screening and treatment", Eye (London, England), 16(1), 33–38
- [8] Retcam, Online:<https://natus.com/products-services/retcam-envision>, Natus Medical Incorporated, Jan 2023.
- [9] MII Ret Cam Inc (Smartphone Based Retina Imaging device), Online: <https://www.medicalsdir.com/listing/mii-ret-cam-inc-smartphone-based-retina-imaging-device/>, Jan 2023.
- [10] Worrall, D. E., Wilson, C. M., & Brostow, G. J., "Automated retinopathy of prematurity case detection with convolutional neural networks.", Lecture Notes in Computer Science (Including Subseries Lecture Notes in Artificial Intelligence and Lecture Notes in Bioinformatics), 10008 LNCS, pp.68–76, 2016.
- [11] Wang, J., Ju, R., Chen, Y., Zhang, L., Hu, J., Wu, Y., ... Yi, Z. (2018). Automated retinopathy of prematurity screening using deep neural networks. *EBioMedicine*, 35, p.361.
- [12] Brown, J. M., Campbell, J. P., Beers, A., Chang, K., Ostmo, S., Chan, R. V. P., ... Chiang, M. F. (2018). Automated Diagnosis of Plus Disease in Retinopathy of Prematurity Using Deep Convolutional Neural Networks. *JAMA Ophthalmology*, 136(7), 803. <https://doi.org/10.1001/JAMAOPHTHALMOL.2018.1934>
- [13] Mulay, S., Ram, K., Sivaprakasam, M., & Vinekar, A., "Early detection of retinopathy of prematurity stage using deep learning approach.", pp.758–764, 2019
- [14] Vinekar, A., Jie, V. Y. W., Savoy, F. M., & Parthasarathy, D. R. (2021). Development and validation of a Deep Learning (DL)-based screening tool for 'Plus disease' detection on retinal images captured through a tele-ophthalmology platform for Retinopathy of prematurity (ROP) in India. *Investigative Ophthalmology & Visual Science*, 62(8), 3267–3267.
- [15] Tong, Y., Lu, W., Deng, Q. qin, Chen, C., & Shen, Y. (2020). Automated identification of retinopathy of prematurity by image-based deep learning. *Eye and Vision*, 7(1), 1–12. <https://doi.org/10.1186/S40662-020-00206-2/TABLES/4>
- [16] Qiaowei Wu, Yijun Hu, Zhenyao Mo, Rong Wu, Xiayin Zhang, Yahan Yang, Baoyi Liu, Yu Xiao, Xiaomin Zeng, Zhanjie Lin, Ying Fang Yijin Wang, Xiaohe Lu, Yanping Song, Wing W. Y. Ng, Songfu Feng, Honghua Yu. (2022). "Development and Validation of a Deep Learning Model to predict the occurrence and severity of Retinopathy of Prematurity", *JAMA Ophthalmology*
- [17] Ding A, Chen Q, Cao Y, Liu B, et al. "Retinopathy of Prematurity Stage Diagnosis Using Object Segmentation and Convolutional Neural Networks." arxiv.org arXiv preprint, 2020
- [18] Zhao J, Lei B, Wu Z, Zhang Y, Li Y, Wang L, Wang T. A deep learning framework for identifying Zone I in RetCam images. *IEEE Access*. 2019;7:103530–103537. doi: 10.1109/ACCESS.2019.2930120
- [19] Zuiderveld, K. "Contrast Limited Adaptive Histogram Equilization.", Academic Press Processional: San Diego, CA, USA, 1994; pp. 474-485.
- [20] Cheng H.D, Shi X.J, "A simple and effective histogram equilisation approach to image enhancement", *Digital Signal Processing*, Vol 14, Issue 2, pp. 158-170.

- [21] O. D. Team, "Histogram equalization," Dec 2019. [Online]. Available: <https://docs.opencv.org/2.4/doc/tutorials/imgproc/histograms/>
- [22] Pizer, M, Amburn P.E, Austin D.J, et al. "Adaptive histogram equalization at its variations", Computer Vision, Graphics, and Image Processing, Vol 39, Issue 3, 1987, pp 355-268.
- [23] M. Usman. Akram, Anam. Tariq, Sarwat. Nasir, and Shoab. Khan "Gabor wavelet based vessel segmentation in retinal images." Computational Intelligence for Image Processing, CIIP, IEEE Symposium on , pp. 116-119, 2009.
- [24] M. Usman. Akram, Anam. Tariq, Shehzad. Khalid, Farooque. Azam, and Shoab. Khan "Detection and classification of retinal lesions for grading of diabetic retinopathy." Computers in Biology and Medicine , Vol. 45, pp. 161-171, Feb 2014.
- [25] Chaudhury S, Krishna N.A, et. Al. "Effective Image Processing and Segmentation-Based Machine Learning Techniques for Diagnosis of Breast Cancer". Computational and Mathematical Methods in Medicine, vol 2022, Article id 6841334, 2022.
- [26] Sinan S, Sheet M., et al. "Retinal disease identification using upgraded CLAHE filter and transfer convolution neural network", ICT Express, Volume 8, Issue 1, 2022, Pages 142-150
- [27] Jabbar MK, Yan J, Xu H, Ur Rehman Z, Jabbar A. Transfer Learning-Based Model for Diabetic Retinopathy Diagnosis Using Retinal Images. *Brain Sci.* 2022 Apr 22;12(5):535. doi: 10.3390/brainsci12050535. PMID: 35624922; PMCID: PMC9139157.
- [28] Gangwar, A.K, Ravi, V., "Diabetic Retinopathy Detection Using Transfer Learning", Evolution in Computational Intelligence. Advances in Intelligent Systems and Computing, Springer, Singapore, vol 1176, 2021.
- [29] K. He, J.Sun, Tang, "Single Image Haze removal using dark channel prior". IEEE International Conference on Computer Vision and Pattern Recognition, 1956-1963, 2009.
- [30] Zhu, Q et al. "Single Image Dehazing Using Color Attenuation Prior", British Machine Vision Conference (2014).
- [31] Sami B.S., Muqeet A., Tariq H., "A Novel Image Dehazing and Assessment Method", 8<sup>th</sup> International Conference on Information and Communication Technologies (ICICT) ppp. 72-77, 2019
- [32] Gaudio, A., Smailagic, A., et al. "Enhancement of Retinal Fundus Images via Pixel Color Amplification", ICIAR 2020, June
- [33] Zhang S., Carroll A.B. Webers, et al, "A double-pass reflection model for efficient single retinal image enhancement", Signal Processing, Nov 2021.
- [34] Dissopa J, Kansomkeat S, Intajag S. "Enhance Contrast and Balance Color of Retinal Image" Symmetry. 2021, Vol 13, Issue 11.
- [35] Olaf. Ronneberger, Philipp. Fischer, and Thomas. Brox. "U-net: Convolutional networks for biomedical image segmentation." In International Conference on Medical Image Computing and Computer Assisted Intervention p. 234-241, Springer 2015.
- [36] Galdran A, Andre A, Dolz J, Chakor H, Lomaert H, Ayed BI, "The Little W-Net That Could: State-of-the-art Retinal Vessel Segmentation with Minimalistic Models", <https://arxiv.org/abs/2009.01907>, Sep. 2020.
- [37] Venturelli M., "The dangers behind image resizing", <https://zuru.tech/blog/the-dangers-behind-image-resizing>, Aug 2021.
- [38] OpenCV, "Geometric Transformations", [https://docs.opencv.org/3.4/da/d54/group\\_\\_imgproc\\_\\_transform.html](https://docs.opencv.org/3.4/da/d54/group__imgproc__transform.html), Dec 2022.
- [39] OpenCV, "Image Processing", [https://docs.opencv.org/3.4/d7/dbd/group\\_\\_imgproc.html](https://docs.opencv.org/3.4/d7/dbd/group__imgproc.html), Dec 2022.
- [40] Keras, "Resnet and Resnetv2", [ResNet and ResNetV2 \(keras.io\)](https://keras.io/api/applications/resnet/), Jan 2023.
- [41] Keras, "InceptionResnetv2", [InceptionResNetV2 \(keras.io\)](https://keras.io/api/applications/inception_resnet_v2/), Jan 2023.
- [42] Keras, "DenseNet", [DenseNet \(keras.io\)](https://keras.io/api/applications/dense/), Jan 2023.
- [43] Keras, "Developer guides/Transfer learning & fine-tuning", [https://keras.io/guides/transfer\\_learning/](https://keras.io/guides/transfer_learning/), June, 2022
- [44] Keras, "Grad Cam", [https://keras.io/examples/vision/grad\\_cam/](https://keras.io/examples/vision/grad_cam/) , Han 2023